Anomalous behavior of nonequilibrium excitations in UO_{2}

Dylan R. Rittman, Samuel W. Teitelbaum, David A. Reis, Wendy L. Mao, and Rodney C. Ewing

Phys. Rev. B **99**, 134307 — Published 22 April 2019

DOI: 10.1103/PhysRevB.99.134307

Anomalous behavior of non-equilibrium excitations in UO_2

Dylan R. Rittman[1], Samuel W. Teitelbaum[2,3], David A. Reis[2,3], Wendy L. Mao[1,3], Rodney C. Ewing[1]

[1] Department of Geological Sciences, Stanford University, Stanford, California 94305, USA

[2] Stanford PULSE Institute, SLAC National Accelerator Laboratory, Menlo Park, California 94025, USA

[3] Stanford Institute for Materials & Energy Sciences, SLAC National Accelerator Laboratory, Menlo Park, California 94025, USA

Ultrafast optical pump-probe studies of uranium dioxide (UO_2) under pressure were performed in order to better understand the material's response to ionizing radiation. Photoexcitation generates oscillations in the time-resolved reflectivity at two distinct GHz-scale frequencies. The higher frequency mode is attributed to a coherent longitudinal acoustic mode. The lower frequency mode does not correspond to any known excitation under equilibrium conditions. The frequency and lifetime of the low-frequency mode are studied as a function of pressure. Abrupt changes in the pressure-dependent slopes of these attributes are observed at ~10 GPa, which correlates with an electronic transition in UO_2. Variation of probe wavelength reveals that the low *k* dispersion of the low-frequency mode does not fit into either an optical or acoustic framework. Rather, we propose that this mode is related to the dynamical magnetic structure of UO_2. The implications of these results help account for the anomalously small volume of damage known to be caused by ionizing radiation in UO_2; we propose that the existence of the low-frequency mode enhances the material's transient thermal conductivity, while its long lifetime lengthens the timescale over which energy is dissipated. Both mechanisms enhance damage recovery.

I. INTRODUCTION

Uranium dioxide (UO_2) is a Mott-Hubbard insulator in which both the lower and upper Hubbard bands are dominated by U *5f* states [1]. UO_2 is important because it is the fuel for nearly all commercial nuclear reactors. Despite its importance as a nuclear material, its response to ionizing radiation is not well understood. Fission of uranium atoms produces high-energy "fission fragments" that deposit their energy primarily into the electronic subsystem of UO_2, producing cylindrical tracks of permanent structural damage that are nanometers wide and microns in length. Notably, the track radii observed in UO_2 are smaller than expected [3], even when compared with materials that have similar thermal and physical properties [3,4]. This has led to different models for the damage process [4,5].

Several models have been put forth in an attempt to understand the process of track formation. Duffy *et al*. [6] and Itoh *et al*. [7] proposed bond-weakening models hypothesizing that electronic excitations change the bonding environment, leading to atomic motion. Toulemonde *et al*. [8] and Szenes [9] proposed thermal spike models positing that local high temperatures, resulting from phonon emission following electron recombination, cause the damage. Ronchi and Wiss [10] and Zhang *et al*. [11] proposed shock wave models suggesting that a high-pressure strain wave generated by the expansion of the excited region of the sample induces plastic deformation. Finally, Baldinozzi *et al*. [12] and Tracy *et al*. [13] proposed point defect models whereby the extreme conditions caused by the fission fragments generate defects that can collectively cause phase transformations.

All of these models represent attempts to understand the behavior of irradiated materials on femtosecond-to-nanosecond timescales through the interpretation of data recorded well-after irradiation. Additionally, the models are either qualitative in their attempts to explain observed

features of radiation damage (*e.g.*, bond-weakening model) or are quantitative but use equilibrium material parameters and empirical fits to explain highly non-equilibrium processes (*e.g.*, thermal spike model). Direct experimental studies of the radiation damage process on the applicable femtosecond-to-nanosecond timescales are needed in order to obtain a solid understanding of the series of processes that eventually lead to the permanent damage state of the material.

Ultrafast laser irradiation has been shown to induce a similar damage process as high-energy ions since both sources deposit their energy though electronic excitations on femtosecond timescales [14-16]. Furthermore, this similar damage process has been shown to induce the same structural phase transformations in the same materials [15]. The ability to temporally resolve ultrafast laser pulses allows one to directly observe the radiation damage process on the relevant timescales by using time-resolved pump-probe spectroscopy.

The response of UO_2 to ultrafast photoexcitation has been investigated previously using a variety of time-resolved probes, including optical reflectivity [17,18], THz spectroscopy [19], and photoemission spectroscopy [20,21]. Ultrafast reflectivity measurements revealed the generation of a coherent longitudinal acoustic (LA) phonon as well as reflectivity oscillations not associated with any Raman-active mode observed under equilibrium conditions [18]. Both of these modes have been proposed to result from the production of photogenerated polarons as excitation drives a charge-transfer transition that induces a mixed-valence state of a U^{3+}/U^{5+} from a pair of U^{4+} sites [18]. However, evidence supporting the specific identification of the photogenerated species as a polaron is limited.

Here, we study the response of single crystal UO_2 to ultrafast photoexcitation by measuring the time-dependent optical reflectivity at high pressure. We observe both the coherent

acoustic phonon and the lower frequency non-equilibrium mode. The frequency and lifetime of these modes as a function of pressure are used to understand how photoexcition couples to the atomic and electronic structure of UO_2. Multiple probe wavelengths are employed in order to determine the dispersion relation of the two modes at low wavevector, k. These results are consistent with a non-equilibrium character of the lower frequency mode, but also cast doubt on the assignment of the photogenerated species as polaronic in nature. These results provide a new basis for the identification of the photogenerated species and help explain the remarkable resistance of UO_2 to ionizing radiation damage.

II. METHODS

Ultrafast optical pump-probe experiments were performed using a Ti:sapphire laser with a pulse duration of 50 fs and central wavelength of 800 nm. The initial beam was split into pump and probe paths, with the pump beam frequency doubled to 400 nm using a beta barium borate crystal in order to excite above the ~2.1 eV band gap of UO_2 [1,22]. A prism compressor was then used to recompress the frequency-doubled pump beam to a 50-fs pulse duration. The pump fluence was varied from 0.75 to 1.50 mJ/cm^2. The probe beam, still at 800 nm, was used to monitor the time-dependent reflectivity of the sample. Probe fluence was over an order of magnitude lower than the pump beam for all measurements. Both the pump and probe were combined collinearly with a dichroic beam splitter, coupled into a microscope objective to focus onto a ~20 μm diameter spot on the UO_2 sample. The probe was collected in reflection mode and directed onto a silicon photodiode to measure reflectivity. The pump-probe signal was detected with a lock-in amplifier and optical chopper. For selected pressures, multiple probe wavelengths were used to better understand the dispersion relation of the modes. To do this, the probe beam

was focused into a sapphire plate to generate a white-light continuum that was then filtered using a holographic band-pass filter to select a specific probe wavelength—either 700 or 900 nm.

The measurements were collected at elevated pressure using a diamond anvil cell (DAC) at room temperature. The DAC generated pressure by compressing the sample between two opposing diamond anvils with 500 μm culet diameter. A tungsten gasket was pre-indented to a thickness of 100 μm, at which point a 200 μm diameter hole was drilled into the center of the pre-indention to serve as the sample chamber. A single crystal of UO_2 was placed into the chamber along with a ruby crystal and the pressure-transmitting medium. Fluorescence from the ruby was used to monitor pressure, with errors in reported values of less than 0.5 GPa. Silicone oil was used as the pressure-transmitting medium to create quasi-hydrostatic conditions [23]. The maximum pressure of the sample was kept below 20 GPa because at higher pressures the band gap narrows below 1.55 eV, causing the 800 nm probe beam to be absorbed through a one-photon process [24], effectively altering the region of the sample being probed.

III. RESULTS

The time-dependent reflectivity traces of photoexcited UO_2 up to 20 GPa are shown in Fig. 1a. The Fourier transform of the time-domain data, following subtraction of an exponentially decaying background, is shown in Fig. 1b. Two GHz-scale modes are identified. The high-frequency mode (HFM) is generated by the sudden laser-induced stress at the surface and detected through stimulated Brillouin scattering of a known LA mode [An 2011]. This LA mode has been well-characterized through inelastic neutron scattering [25], ultrasonic measurements [26], and computational work [27], so the detection of the HFM is expected. The low-frequency mode (LFM) results from the creation of photogenerated species [18] and is notably not observed through measurements of UO_2 at equilibrium conditions. To date, the

identity of this photogenerated species is poorly understood, and its behavior poorly characterized.

The pressure-dependent frequencies of both modes are shown in Fig. 2. The HFM hardens gradually and continuously over the entire pressure range. As expected, its hardening rate matches the pressure-induced increase in UO_2 longitudinal sound speed [28]. Interestingly, the LFM displays an anomalous non-linear response to pressure. The frequency of the mode increases rapidly—much faster than contributions from increasing sound speed can account for—until ~10 GPa. Above ~10 GPa, the rate of hardening slows as pressure continues to increase. No relation between frequency and incident pump fluence was observed, and scatter in frequency for different pump fluences was less than 0.5 GHz.

Oscillations in the time-domain data are fit to a sum of two exponentially decaying sinusoids. For the LFM, the time constant of the decay acts as a lower bound for the lifetime of the photogenerated species. The pressure-dependent LFM lifetime is shown in Fig. 3. The lifetime decreases as pressure increases to ~10 GPa, at which point it levels off as pressure continues to increase. This behavior is similar to the observed trend in LFM frequency (Fig. 2), where there are distinct behaviors between the low- and high-pressure regimes. Notably, LFM frequency and lifetime are coupled such that their product is constant at a value of ~5. Lifetime is found to be invariant with pump fluence indicating that, at these fluences, interactions between the photogenerated species causing decay are negligible [17].

There is an abrupt change in the pressure-dependent slope of both the LFM frequency and lifetime at ~10 GPa. However, there are no structural phase transformations in UO_2 in the studied pressure range [24,29]. This means that there is no strong correlation between LFM behavior and the atomic structure of UO_2, which suggests that the photogenerated species is not

coupled to the atomic structure of the UO_2. Notably, there is a change in the electronic structure of UO_2 at ~10-15 GPa. Transitions within the $5f^2$ multiplet levels are allowed due to increasing admixture of the *d*-band into the $5f^2$ ground state [30,31]. The multiplet energy levels involved in these transitions are a consequence of spin-orbit coupling in UO_2 [32]. Furthermore, the pressure-induced electronic transition has been found to coincide with a rapid decrease in resistivity [24]. The correlation between electronic transitions in UO_2 and change in LFM behavior implies a coupling between the photogenerated species and the electronic structure of UO_2. This is consistent with previous work that showed that the LFM lifetime depends on the energy level to which the electrons were initially excited [18].

The rapid and non-linear pressure-dependent frequency shift of the LFM is uncharacteristic of an acoustic phonon mode, whose hardening as a function of pressure should be dominated by an increase in the sound speed, and its GHz-scale frequency is unexpected for an optical phonon mode. In order to better understand the character of the LFM, measurements were performed at additional probe wavelengths to understand the mode's dispersion relation at low *k*, which is a function of the known probe wavelength (λ) and the previously measured refractive index (n) at the probe wavelength [33], where $k = 4\pi n/\lambda$. At low *k*, acoustic modes should be linear with *k* through the origin, while optical modes should be constant with *k*.

Mode frequency as a function of *k* is shown in Fig. 4. Results are shown for pressures both below and above the ~10 GPa electronic transition. In both cases, the HFM, known to be an LA phonon, displays the expected linear variation with *k*. The LFM, on the other hand, varies slowly and nonlinearly with *k* in a way not expected for either acoustic or optical phonons at such low wavevector. Chi-square tests showed that the HFM fit the acoustic phonon model at both pressures to a significance of $p < 0.05$. However, the LFM did not fit either the acoustic or

optical phonon models at both pressures, which supports the characterization of its low *k* dispersion as "non-linear."

IV. DISCUSSION

Previous work on photogenerated species in a variety of other materials have shown that polarons and excitons typically produce acoustic phonons [34-36] due to the volumetric expansion caused by the excited-state quasiparticles. These quasiparticle-related acoustic modes were differentiated from acoustic modes produced by simple carrier excitation or thermal expansion through *in situ* charge measurement [34], response to magnetic transitions [35], and correlation of mode frequency with quasiparticle size [36]. Notably, neither the pressure dependence nor dispersion relation of the LFM indicates an acoustic response, meaning it would be atypical for the source of the LFM to be photoinduced polarons as proposed previously [18].

Another possible explanation for the origin of the LFM is that it is a local electronic excitation that interacts with the HFM upon increasing pressure. This interaction could explain the change in the pressure-dependent slope of the LFM frequency. However, a local electronic excitation would be expected to produce THz-scale optical phonons and have a corresponding ground-state mode [36,37]. This is inconsistent with the observed frequency and dispersion of the LFM, as well as the fact that there is no corresponding ground-state mode for the LFM.

An alternative explanation for the origin of the LFM is related to the magnetic structure of UO_2. Previous investigations into photoexcited magnetic materials have shown that modes originating from coherently-generated magnons also exhibit GHz-scale frequencies [38,39]. Furthermore, these frequencies change with probe wavelength, though not according to the Brillouin process expected by acoustic phonons. Magnons are collective excitations that can

occur in magnetically ordered materials as temporally and spatially dependent magnetic ordering. This changing order can manifest in the material's optical properties by the coupling of magnetic ordering to the material's optical properties [39]. Notably, UO_2, with a Néel temperature of 30.8 K, is paramagnetic (magnetically disordered) at room temperature. This differs from previous work on coherently-generated magnons in rare-earth doped $BiFeO_3$, which observed the loss of the one-magnon mode above the Néel temperature [38]. However, local, uncorrelated magnetic distortions caused by a dynamical Jahn-Teller effect have been observed in UO_2 above the Néel temperature [40]. Thus, it is possible that ultrafast photoexcitation could generate coherent magnons even within paramagnetic UO_2. We note that we do not have direct evidence for this interpretation and therefore view this as a speculative hypothesis. However, while the relation between the LFM and dynamical magnetic order in UO_2 is not conclusive, it is consistent with experimental results presented here and in other work.

These results have important implications for understanding the ionizing radiation damage process in UO_2. The long lifetime of the LFM means that the existence of photogenerated species effectively lengthens the timescale over which energy deposited by ionizing radiation is dissipated through the material [41]. Furthermore, a new energy-loss channel open to UO_2 during a radiation event can effectively increase its thermal conductivity during the transient radiation damage process [42]. Both of these mechanisms enhance recovery of the damaged domains and may account for the anomalously small amount of damage observed in UO_2 due to ionizing radiation. More broadly, these results illustrate that accurately modeling radiation damage requires identifying and understanding non-equilibrium processes rather than extrapolating equilibrium properties to short timescales, and that highly excited UO_2 has energy-loss pathways that are not observable under equilibrium conditions.

V. CONCLUSION

UO_2 was subjected to ultrafast photoexcitation at high pressure. Time-dependent reflectivity measurements revealed two oscillatory modes of GHz-scale frequencies. The HFM was identified as a well-known LA mode and its behavior to high pressure was consistent with this assignment. Conversely, the LFM, which did not correspond to any known excitation under equilibrium conditions, was found to have anomalous behavior at high pressure. This included an abrupt change in the pressure-dependent slopes of its frequency and lifetime, which were found to correlate with an electronic transition in UO_2. Furthermore, varying the wavelength of the probe pulse revealed non-linear dispersion of the LFM at low *k*. These behaviors were found to be inconsistent with the previous hypothesis that the LFM is of polaronic origin. Rather, these behaviors were found to be consistent with a magnetic origin of the LFM, though this conclusion is speculative.

ACKNOWLEDGEMENTS

This work was supported as part of "Materials Science of Actinides", an Energy Frontier Research Center funded by the U.S. Department of Energy (DOE) Office of Science, Basic Energy Sciences (Grant No. DE-SC0001089). S.W.T. and D.A.R. were funded by the DOE Office of Science, Office of Basic Energy Sciences through the Division of Materials Sciences and Engineering under Contract No. DE-AC02-76SF00515.

REFERENCES

[1] S. W. Yu, J. G. Tobin, J. C. Crowhurst, S. Sharma, J. K. Dewhurst, P. Olalde-Velasco, W. L. Yang, and W. J. Siekhaus, *Phys. Rev. B* **83**, 165102 (2011).

[2] M. Toulemonde, A. Benyagoub, C. Trautmann, N. Khalfaoui, M. Boccanfuso, C. Dufour, F. Gourbilleau, J. J. Grob, J. P. Stoquert, J. M. Costantini, F. Haas, E. Jacquet, K.-O. Voss, and A. Meftah, *Phys. Rev. B* **85**, 054112 (2012).

[3] T. Sonoda, M. Kinoshita, N. Ishikawa, M. Sataka, A. Iwase, and K. Yasunaga, *Nucl. Instrum. Methods Phys. Res., Sect. B* **268**, 3277 (2010).

[4] N. Ishikawa, T. Sonoda, T. Sawabe, H. Sugai, and M. Sataka, *Nucl. Instrum. Methods Phys. Res., Sect. B* **314**, 180 (2013).

[5] G. Szenes, *J. Nucl. Mat.* **482**, 28 (2016).

[6] D. M. Duffy, S. L. Daraszewicz, and J. Mulroue, *Nucl. Instrum. Methods Phys. Res., Sect. B* **277**, 21 (2012).

[7] N. Itoh, D. M. Duffy, S. Khakshouri, and A. M. Stoneham, *J. Phys.: Condens. Matter* **21**, 474205 (2009).

[8] M. Toulemonde, C. Dufour, and E. Paumier, *Phys. Rev. B* **46**, 14362 (1992).

[9] G. Szenes, *Phys. Rev. B* **51**, 8026 (1995).

[10] C. Ronchi and T. Wiss, *J. Appl. Phys.* **92**, 5837 (2002).

[11] J. Zhang, M. Lang, R. C. Ewing, R. Devanathan, W. J. Weber, and M. Toulemonde, *J. Mat. Res.* **25**, 1344 (2010).

[12] G. Baldinozzi, D. Simeone, D. Gosset, I. Monnet, S. Le Caër, and L. Mazerolles, *Phys. Rev. B* **74**, 132107 (2006).

[13] C. L. Tracy, M. Lang, F. X. Zhang, C. Trautmann, and R. C. Ewing, *Phys. Rev. B* **92**, 174101 (2015).

[14] B. Rethfeld, A. Rämer, N. Brouwer, N. Medvedev, and O. Osmani, *Nucl. Instrum. Methods Phys. Res., Sect. B* **327**, 78 (2014).

[15] D. R. Rittman, C. L. Tracy, A. B. Cusick, M. J. Abere, B. Torralva, R. C. Ewing, and S. M. Yalisove, *Appl. Phys. Lett.* **106**, 171914 (2015).

[16] D. R. Rittman, C. L. Tracy, C. H. Chen, J. M. Solomon, M. Asta, W. L. Mao, S. M. Yalisove, and R. C. Ewing, *Phys. Rev. B* **97**, 024104 (2018).

[17] Y. Q. An, A. J. Taylor, S. D. Conradson, S. A. Trugman, T. Durakiewicz, and G. Rodriguez, *Phys. Rev. Lett.* **106**, 207402 (2011).

[18] S. D. Conradson, T. Durakiewicz, F. J. Espinosa-Faller, Y. Q. An, D. A. Andersson, A. R. Bishop, K. S. Boland, J. A. Bradley, D. D. Byler, D. L. Clark, D. R. Conradson, L. L. Conradson, A. L. Costello, N. J. Hess, G. H. Lander, A. Llobet, M. B. Martucci, J. Mustre de Leon, D. Nordlund, J. S. Lezama-Pacheco, T. E. Proffen, G. Rodriguez, D. E. Schwarz, G. T. Seidler, A. J. Taylor, S. A. Trugman, T. A. Tyson, and J. A. Valdez, *Phys. Rev. B* **88**, 115135 (2013).

[19] S. D. Conradson, S. M. Gilbertson, S. L. Daifuku, J. A. Kehl, T. Durakiewicz, D. A. Andersson, A. R. Bishop, D. D. Byler, P. Maldonado, P. M. Oppeneer, J. A. Valdez, M. L. Neidig, and G. Rodriguez, *Sci. Rep.* **5**, 15278 (2015).

[20] S. M. Gilbertson, T. Durakiewicz, G. L. Dakovski, Y. Li, J. X. Zhu, S. D. Conradson, S. A. Trugman, and G. Rodriguez, *Phys. Rev. Lett.* **112**, 087402 (2014).

[21] S. D. Conradson, D. A. Andersson, K. S. Boland, J. A. Bradley, D. D. Byler, T. Durakiewicz, S. M. Gilbertson, S. A. Kozimor, K. O. Kvashnina, D. Norlund, G. Rodriguez, G. T. Seidler, P. S. Bagus, S. M. Butorin, D. R. Conradson, F. J. Espinosa-Faller, N. J. Hess, J. J. Kas, J. S. Lezama-Pacheco, P. Martin, M. B. Martucci, J. J. Rehr, J. A. Valdez, A. R. Bishop, G. Baldinozzi, D. L. Clark, and A. Tayal. *Phys. Rev. B* **96**, 125114 (2017).

[22] J. Schoenes, *J. Appl. Phys.* **49**, 1463 (1978).

[23] S. Klotz, J. C. Chervin, P. Munsch, and G. Le Marchand, *J. Phys. D: Appl. Phys.* **42**, 075413 (2009).

[24] J. C. Crowhurst, J. R. Jeffries, D. Åberg, J. M. Zaug, Z. R. Dai, W. J. Siekhaus, N. E. Teslich, K. S. Holliday, K. B. Knight, A. J. Nelson, and I. D. Hutcheon, *J. Phys.: Condens. Matter* **27**, 265401 (2015).

[25] G. Dolling, R. A. Cowley, and A. D. Woods, *Can. J. Phys.* **43**, 1397 (1965).

[26] J. P. Panakkal and J. K. Ghosh, *J. Mater. Sci. Lett.* **3**, 835 (1984).

[27] M. Sanati, R. C. Albers, T. Lookman, and A. Saxena, *Phys. Rev. B* **84**, 014116 (2011).

[28] B. T. Wang, P. Zhang, R. Lizárraga, I. Di Marco, O. Eriksson, *Phys. Rev. B* **88**, 104107 (2013).

[29] D.R. Rittman, S. Park, C. L. Tracy, L. Zhang, R. I. Palomares, M. Lang, A. Navrotsky, W. L. Mao, and R. C. Ewing, *J. Nucl. Mat.* **490**, 28 (2017).

[30] U. Benedict, *J. Alloys Compd.* **213**, 153 (1994).

[31] K. Syassen, H. Winzen, and U. Benedict, *Physica B* **144**, 91 (1986).

[32] H. Ramanantoanina, G. Kurim C. Daul, and J. Bertsch, *Phys. Chem. Chem. Phys.* **18**, 19020 (2016).

[33] R. J. Ackermann, R. J. Thorn, and G. H. Winslow, *J. Opt. Soc. Am.* **49**, 1107 (1959).

[34] B. B. Zhang, J. Liu, X. Wei, D. R. Sun, Q. J. Jia, Y. Li, and Y. Tao, *Appl. Phys. Lett.* **110**, 151904 (2017).

[35] Y. H. Ren, M. Trigo, R. Merlin, V. Adyam, and Q. Li, *Appl. Phys. Lett.* **90**, 251918 (2007).

[36] F. X. Morrissey, J. G. Mance, A. D. Van Pelt, and S. L. Dexheimer, *J. Phys.: Condens. Matter* **25**, 144204 (2013).

[37] F. X. Morrissey, Ph.D. thesis, Washington State University, 2007.

[38] K. I. Doig, F. Aguesse, A. K. Axelsson, N. M. Alford, S. Nawaz, V. R. Palkar, S. P. P. Jones, R. D. Johnson, R. A. Synowicki, and J. Lloyd-Hughes, *Phys. Rev. B* **88**, 094425 (2013).

[39] D. Talbayev, S. A. Trugman, A. V. Balatsky, T. Kimura, A. J. Taylor, and R. D. Averitt, *Phys. Rev. Lett.* **101**, 097603 (2008).

[40] R. Caciuffo, G. Amoretti, P. Santini, G. H. Lander, J. Kulda, and P. de V. Du Plessis, *Phys. Rev. B* **59**, 13892 (1999).

[41] L. Desgranges, G. Baldinozzi, P. Ruello, and C. Petot, *J. Nucl. Mat.* **420**, 334 (2012).

[42] J. W. L. Pang, W. J. L. Buyers, A. Chernatynskiy, M. D. Lumsden, B. C. Larson, and S. R. Phillpot, *Phys. Rev. Lett.* **110**, 157401 (2013).

FIGURES

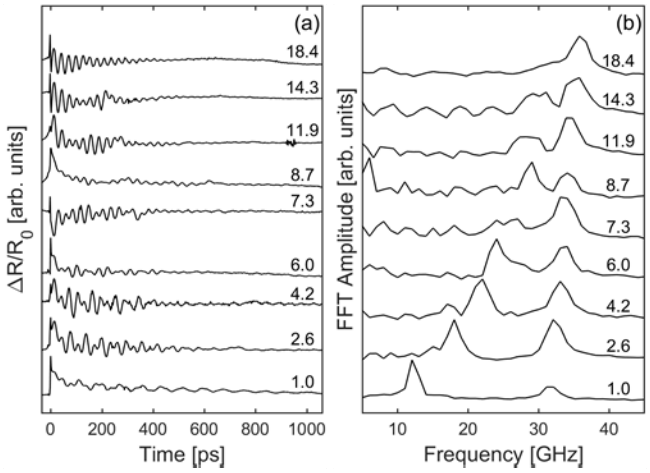

FIG. 1. (a) Time-resolved reflectivity of UO_2 at 800 nm at a variety of pressures (listed on the right in GPa) following ultrafast photoexcitation at 400 nm. (b) Fourier transforms of the traces in (a) following background subtraction. The HFM is attributed to a well-characterized LA phonon, while the LFM results from photogenerated species.

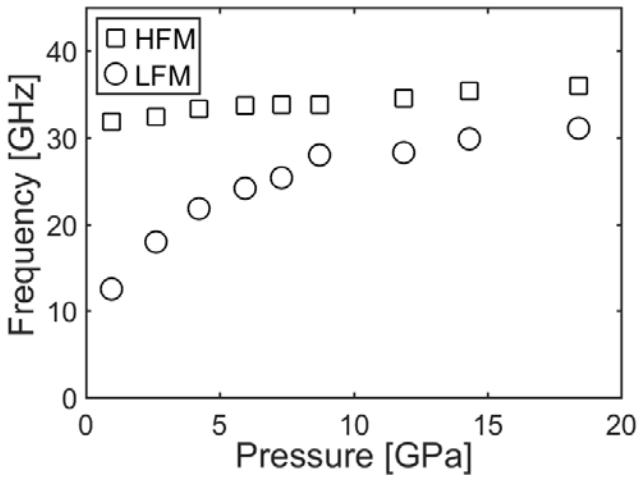

FIG. 2. Frequency of the two observed modes as a function of pressure for 400 nm pump and 800 nm probe pulses. The slight hardening of the HFM is consistent with increased sound velocity at high pressure. The LFM hardens dramatically with pressure up to ~10 GPa, then levels-off as pressure continues to increase. Scatter in frequency values as a function of pump fluence is within the size of the data points. No variation in the frequency is observed as a function of pump fluence.

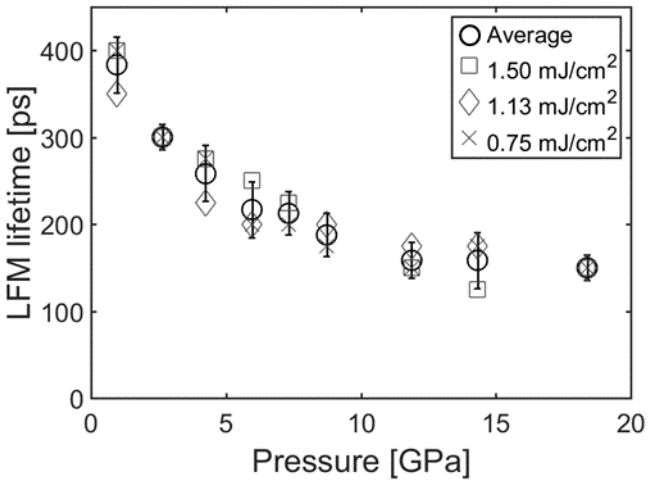

FIG. 3. LFM lifetime as a function of pressure measured with 800 nm probe following ultrafast photoexcitation at 400 nm. Lifetime decreases with increasing pressure up to ~10 GPa, at which point it levels off as pressure continues to increase. LFM lifetime represents the lower bound of the lifetime of the photogenerated species. No systematic trend is observed in the LFM lifetime as a function of pump fluence, only random scatter.

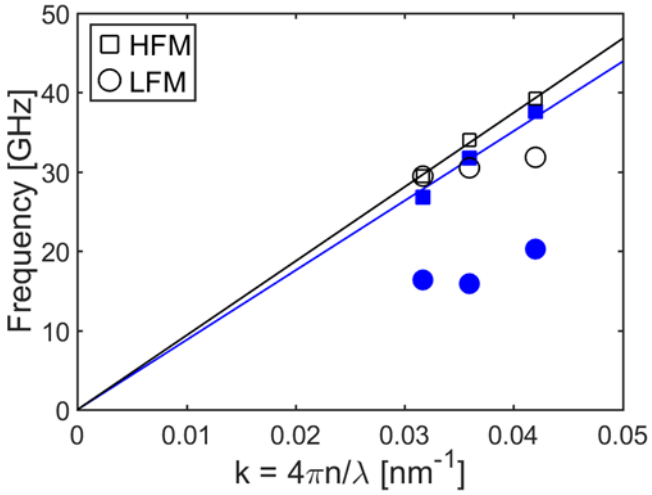

FIG. 4. Color online. Phonon dispersion at low *k*. Probe wavelengths used were 700, 800, and 900 nm. Data in blue (filled) were collected at 2.2 GPa. Data in black (empty), at 12.7 GPa. Error in the data is within the size of the symbols. The frequency of the HFM varies linearly with *k* through the origin, as expected for an acoustic mode. The LFM frequency varies non-linearly with *k*. Wavelength dependent refractive indices are taken from [33].